# Dynamic Model Simulations using Real World Measurements in a Wind Power Generator

JOSÉ VISSIO[1], ANDRÉS GARCÍA[2]

[1]Universidad Tecnológica Nacional, Facultad Regional Bahía Blanca
Departamento de Ingeniería Eléctrica
Bahía Blanca, Buenos Aires
ARGENTINA

[2]Universidad Tecnológica Nacional, Facultad Regional Bahía Blanca
Departamento de Ingeniería Eléctrica, Grupo de Estudios sobre Energía (GESE)
Bahía Blanca, Buenos Aires
ARGENTINA

*Abstract:* In the wind energy sector, one of the most widely used powertrain configurations is the hub-gearbox-doubly fed asynchronous generator. To keep the generator synchronized and connected to the grid, the work performed by the frequency converter and the pitch control system is of utmost importance. Together, they achieve the maximum possible torque—within certain safety parameters—for the available wind resource. This publication presents a simulated pitch control option using actual turbine measurements. The numerical research shows the necessity for nonlinear controllers by showing the linear local uncontrollability of the linearized version.

*Key-Words:* Wind turbine; mechanical model; pitch control; torque control, controllability.

Received: February 12, 2025. Revised: March 27, 2025. Accepted: May 21, 2025. Published: July 14, 2025.

## 1 Introduction

Current wind power generation involves the application of two major areas of engineering: mechanical and electrical/electronic, [1], [2]. In this sense, while the reception of wind energy is optimized with increasingly desirable advanced blade and gearbox designs, once a rotating shaft is established, that mechanical energy is converted into electrical energy, mostly through double fed asynchronous generators as shown Fig 1. In any case, it is clear that the ultimate goal is to inject the harvested electrical energy into the HV grid, for which synchronization of both frequency and voltage is necessary.

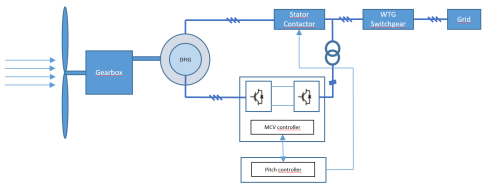


Figure 1: DFIG configuration

Currently, although there are several ways to control the kinetic energy extracted from the wind, the most common is through pitch control, either individually or as a whole, [3] [4], [5], [6]. Failure to implement this control would force the wind turbine to meet the necessary electrical conditions (imposed by the grid to which they will be connected) to be able to inject the generated power only in very small wind speed windows. In order to broaden the spectrum in which grid conditions are achieved two actions are required. A specific signal is injected into the generator rotor — using a frequency converter — and blade angle is optimized by measuring the main shaft torque.

Different studies have been published that seek to control the variables blade angle and torque in generator's shaft by using different techniques, [7],[8]. Based on proposed models, a linearization option for control equations is added. To evaluate the results, values taken from an operating turbine and its corresponding parameters are entered to assess the performance and results.

## 2 Problem Formulation

A turbine's control system is affected by various nonlinearities that it must overcome in order to continue supplying electrical energy to the grid, [9]. The control system must maintain specific

conditions imposed by the electrical grid and absorb its fluctuations within certain limits. In turn, the raw material from which the energy conversion is carried out also fluctuates, presenting the control system with different scenarios at each moment in time. It is essential to have a robust control system that can react in a timely manner by controlling the generator's torque and blade angle to avoid generating excessive stress on equipment such as blades, main shaft, and gearbox, as well as to avoid losing synchronization with the electrical grid.

# 3 Problem Statement

## 3.1 Working zones

To keep the generator synchronized with the power grid, a wind turbine has two control modes depending on the available raw material and the generator's rotational speed. Therefore, three theoretical operating zones are considered, see Fig 2:

- Undersynchronization: The resource is low, so the blades are pitched at values close to 0° using pitch control to maximize the conversion of wind kinetic energy to mechanical energy on the main shaft. In this way, the balance of generated torque and resistive torque allows the generator to reach a speed that, when combined with a low frequency injected by the frequency converter into the generator rotor, allows it to reach the nominal grid frequency, synchronize with it, and inject power.

- Synchronous: The device transmits torque to the power train that allows it to rotate at synchronous speed. The frequency converter injects a direct current into the rotor. This area is not used in practice due to the generator used and its control difficulties.

- Hyper-synchronism: The resource is high, so the blade angle is regulated using pitch control to limit torque values in the powertrain, avoiding overexertion. The frequency converter injects a signal into the rotor to adjust the slip and allow the stator to deliver frequency and rated power. In this working range, the pitch angle is constantly corrected.

**Note:** As a horizontal axis wind turbine blade design method, in any of these operating zones, the power converter continuously corrects the signal at the generator rotor to allow it to remain connected to the grid via a power transformer. In turn, the pitch system regulates the blade angle depending on the resource to maintain optimal torque values on the main shaft.

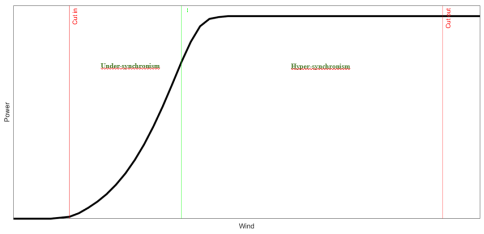


Figure 2: WTG power curve

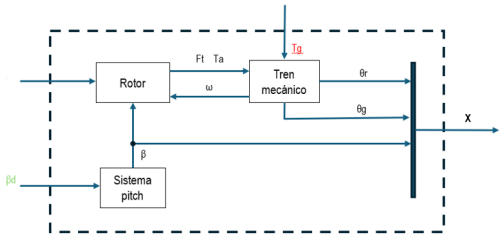


Figure 3: WTG control system

## 3.2 Proposed wind turbine model

The basic operating principle of a wind turbine is to extract the kinetic energy of the wind through the blades and transform it into torque in the drive train as illustrated in Fig 3. This is how the wind ($v$) exerts a force on the blades ($F_T$), which extract their kinetic energy by transforming it into torque on the hub shaft ($T_a$). This signal oscillates depending on the applied blade angle, instantaneous variations in wind speed, and the rotational speed of the power train.

Where $v$ is the wind speed (disturbance signal) and $\beta$ is the pitch angle command (control signal). On the other hand, for the pitch command + actuation delay: $F_t$ is the powertrain force, $T_a$ is the powertrain torque, $\omega$ is the power trains' angular velocity, $\theta_r$ is the mechanical's train angular position, $T_g$ is the generator's torque (control signal) and $\theta_g$ is the angular position of the generator shaft.

## 3.3 Drive train model

The powertrain is composed of masses that entail large moments of inertia. The diagram shows the blades, hub, main shaft, gearbox ($Jr$), and the moment of inertia of the generator ($Jg$). The latter, when delivering power to the electrical grid, exerts a resistive torque on the main shaft as describe in (1) and (2):

$$\begin{cases} E_k \\ = \frac{1}{2}m_T\dot{y}_T^2 + \frac{1}{2}Nm_B(\dot{y}_T + \dot{y}_B)^2 + \frac{1}{2}J_r\dot{\theta}_r^2 + \frac{1}{2}J_g\dot{\theta}_g^2 \\ E_p \\ = \frac{1}{2}k_T y_T^2 + \frac{1}{2}Nk_B y_B^2 + \frac{1}{2}d_s(\theta_r - \frac{1}{n_g}\theta_g)^2 \end{cases} \quad (1)$$

$$P_d = \frac{1}{2}d_T\dot{y}_T^2 + \frac{1}{2}Nd_B\dot{y}_B^2 + \frac{1}{2}d_s(\dot{\theta}_r - \frac{1}{n_g}\dot{\theta}_g)^2 \quad (2)$$

Using Lagrangian mechanics:

$$\frac{d}{dt}(\frac{\partial L}{\partial \dot{q}_l}) - \frac{\partial L}{\partial q_I} = f_i - \frac{\partial P_D}{\partial \dot{q}_I}$$

The power train model is obtained in (3):

$$\begin{cases} (m_T + Nm_B)\ddot{y}_T + Nm_B\ddot{y}_B + d_T\dot{y}T + k_T y_T \\ \qquad = F_T \\ Nm_B\ddot{y}_T + Nm_B\ddot{y}_B + Nd_B\dot{y}_B + Nk_B y_B \\ \qquad = F_T \\ J_r\ddot{\theta}_r + d_s(w_r - \frac{1}{n_g}w_g) - k_s(\theta_r - \frac{1}{n_g}\theta_g) \\ \qquad = T_a \\ J_r\frac{1}{n_g}\ddot{\theta}_g - d_s(w_r - \frac{1}{n_g}w_g) - k_s(\theta_r - \frac{1}{n_g}\theta_g) \\ \qquad = -T_g \end{cases} \quad (3)$$

Where $\{m_T, m_B, N, d_T, d_B, k_T, k_B, d_s, n_g\}$ are constants.

### 3.4 Aerodynamic model

The aerodynamics for the blades is described in (4):

$$\begin{cases} F_T &= F_{st}C_T(\lambda, \beta) \\ T_a &= F_{st}RC_Q(\lambda, \beta) \end{cases} \quad (4)$$

Where $C_T$ and $C_Q$ are functions depending on aerodynamic properties of the blades. On the other hand:

$$\lambda = \frac{w_r R}{v}, \quad F_{st} = \frac{1}{2}\rho\pi R^2 v^2$$

The next section describes the complete wind turbine model by joining together (3) and (4).

### 3.5 Complete model

The model in (3) can be re-casted in the following way:

$$\begin{bmatrix} m_T + N\cdot m_B & N\cdot m_B & 0 & 0 \\ N\cdot m_B & N\cdot m_B & 0 & 0 \\ 0 & 0 & J_r & 0 \\ 0 & 0 & 0 & \frac{J_r}{n_g} \end{bmatrix} \cdot \begin{bmatrix} \ddot{y}_T \\ \ddot{y}_B \\ \ddot{\theta}_r \\ \ddot{\theta}_g \end{bmatrix} + \\ + \begin{bmatrix} d_T\cdot\dot{y}_T + k_T\cdot y_T \\ N\cdot d_B\cdot y_B + N\cdot k_B\cdot y_B \\ d_s\cdot(\dot{\theta}_r - \frac{\dot{\theta}_g}{n_g}) - k_s\cdot(\theta_r - \frac{\theta_g}{n_g}) \\ -d_s\cdot(\dot{\theta}_r - \frac{\dot{\theta}_g}{n_g}) - k_s\cdot(\theta_r - \frac{\theta_g}{n_g}) \end{bmatrix} = \begin{bmatrix} F_T \\ F_T \\ T_a \\ -T_g \end{bmatrix}$$

In matrix form:

$$M\cdot Z + B_1\cdot Z + B_2\cdot\dot{Z} = h(v,\beta) + B_3\cdot T_g \quad (5)$$

Where $Z = [y_T, y_B, \theta_r, \theta_g]'$ with the following matrices defined (see (4)):

$$\begin{cases} M = \begin{bmatrix} m_T + N\cdot m_B & N\cdot m_B & 0 & 0 \\ N\cdot m_B & N\cdot m_B & 0 & 0 \\ 0 & 0 & J_r & 0 \\ 0 & 0 & 0 & \frac{J_r}{n_g} \end{bmatrix} \\ B_1 = \begin{bmatrix} k_T & 0 & 0 & 0 \\ 0 & N\cdot k_B & 0 & 0 \\ 0 & 0 & -k_s & \frac{k_s}{n_g} \\ 0 & 0 & -k_s & \frac{k_s}{n_g} \end{bmatrix} \\ B_2 = \begin{bmatrix} d_T & 0 & 0 & 0 \\ 0 & N\cdot d_B & 0 & 0 \\ 0 & 0 & d_s & -\frac{d_s}{n_g} \\ 0 & 0 & -d_s & \frac{d_s}{n_g} \end{bmatrix} \\ h(v,\beta) = \begin{bmatrix} \frac{1}{2}\rho\pi R^2 v^2\cdot C_T(\frac{\dot{\theta}_r\cdot R}{v}, \beta) \\ \frac{1}{2}\rho\pi R^2 v^2\cdot C_T(\frac{\dot{\theta}_r\cdot R}{v}, \beta) \\ \frac{1}{2}\rho\pi R^2 v^2\cdot C_Q(\frac{\dot{\theta}_r\cdot R}{v}, \beta) \\ 0 \end{bmatrix} \quad B_3 = \begin{bmatrix} 0 \\ 0 \\ 0 \\ -1 \end{bmatrix} \end{cases} \quad (6)$$

Writing this system using (5) and (6) in state-space form:

$$\dot{X} = A\cdot X + g(v,\beta) + B\cdot T_g \quad (7)$$

Where $X = [\dot{Z}, Z]'$ and with the following matrices defined:

$$A = \begin{bmatrix} A_1 & A_2 \\ -M^{-1}\cdot B_1 & -M^{-1}\cdot B_2 \end{bmatrix}$$

$$A_1 = \begin{bmatrix} 0 & 1 & 0 & 0 \\ 0 & 0 & 1 & 0 \\ 0 & 0 & 0 & 1 \\ 0 & 0 & 0 & 0 \end{bmatrix}$$

$$A_2 = \begin{bmatrix} 0 & 0 & 0 & 0 \\ 0 & 0 & 0 & 0 \\ 0 & 0 & 0 & 0 \\ 1 & 0 & 0 & 0 \end{bmatrix}$$

$$B = \begin{bmatrix} 0 \\ 0 \\ 0 \\ M^{-1}B_3 \end{bmatrix}$$

The nonlinear term arises:

$$g(x,v) = \begin{bmatrix} 0 \\ 0 \\ 0 \\ M^{-1}\cdot h(v,\beta) \end{bmatrix} \quad (8)$$

### 3.6 Complete model linearization

In order to linearize the model (7), especially the non-linear term (8), the classical method of Taylor series will be used around the equilibrium point (9):

$$\begin{cases} X^A = \begin{bmatrix} y_T \\ y_B \\ \theta_r \\ \theta_g \\ \dot{y_T} \\ \dot{y_B} \\ \dot{\theta_r} \\ \dot{\theta_g} \end{bmatrix} = \begin{bmatrix} 0 \\ 0 \\ 0 \\ 0 \\ 0 \\ 0 \\ 2500 \\ 20 \end{bmatrix} \\ \beta = 3.5 \\ T_g^A = 25 \\ v = 10 \end{cases} \tag{9}$$

Then, the non-linear term (8) can be easily linearized considering as constant functions $C_T$ and $C_Q$:

$$g_{(v,\beta)} \approx g(10, 3.5)$$

Considering:

$$\begin{cases} \tilde{X}_{(t)} = (X_{(t)} - X^A) \rightarrow \dot{\tilde{X}}_{(t)} = \dot{X}_{(t)} \\ \tilde{T_g} = T_g - T_g^A \end{cases}$$

Then:

$$\dot{\tilde{X}}_{(t)} = A(\tilde{X}_{(t)} + X^A) + B(\tilde{T_g} + T_g^A) + g(10, 3.5)$$

Finally:

$$\begin{cases} \dot{\tilde{X}}_{(t)} = A\tilde{X}(t) + B\tilde{T_g} + \underbrace{\left(AX^A + BT_g^A + g(10, 3.5)\right)}_{L} \\ \tilde{Y} = C(\tilde{X} + X^A) \end{cases}$$

Then, the complete linearized model is described in (10):

$$\begin{cases} \dot{\tilde{X}}_{(t)} = \bar{A}\tilde{X} + B\tilde{T_g} + L \\ \tilde{Y} = C\tilde{X} + CX^A \end{cases} \tag{10}$$

**Note:** Matrix $C$ can be considered differently depending on the simulation objectives. In the next section, only one state will be considered as a measured output $\dot{\theta}_g$.

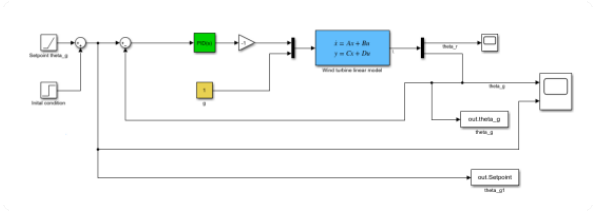

Figure 4: Simulink block diagram using a PID

## 4 Matlab-Simulink simulations

Using a PID controller on the linearized model (10), the Simulink block diagram is depicted in Fig. 4:

Even when a partial tracking for the setpoint can be achieved, it is a very important issue to analyze the controllability matrix $Ctrb$ using the linear model (10):

$$Ctrb = \begin{bmatrix} BA \cdot B \dots A^7 \cdot B \end{bmatrix}$$

which in this case possesses $rank = 2$. In fact, only the states $\theta_r$ and $\theta_g$ can be controlled using only $T_g$, as shown in the following transfer functions:

$$\begin{cases} G_1(s) = \frac{\theta_r(s)}{Tg(s)} = \frac{-3.098 \cdot 10^{-7}}{s^2 + 6 \cdot 10^{-5} \cdot s + 4.066 \cdot 10^{-25}} \\ G_2(s) = \frac{\theta_g(s)}{Tg(s)} = \frac{-s - 3 \cdot 10^{-5}}{s^2 + 6 \cdot 10^{-5} \cdot s + 4.066 \cdot 10^{-25}} \end{cases} \tag{11}$$

Since the system is not completely controllable, the uncontrollable modes must be studied, so the eigenvalues of matrix $A$ arise: $\{-1.4700 + 0.0000i, -0.4264 + 1.3763i, -0.4264 - 1.3763i, 1.1333 + 0.8068i, 1.1333 - 0.8068i, -0.0074 + 0.0000i, 0, 0\}$.

**Note:** Two uncontrollable eigenvalues (modes) are unstable, so the system (linearized) is completely uncontrollable.

A simulation using a PID controller can be depicted in Fig. 5:

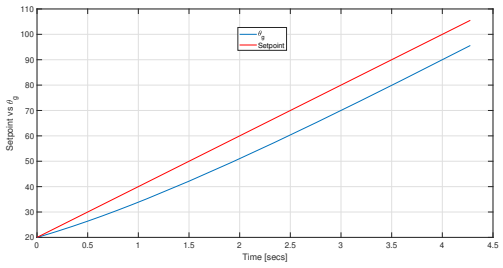


Figure 5: Divergence between setpoint and $\theta_g$ using a PID controller

# 5 Discussion

The analysis and research in this paper using a linearized model and Matlab-Simulink simulations, reveals the following important conclusions:

- With a constant control $\beta$, the linearized system (10) is completely uncontrollable
- Locally, the non-linear model (7) is completely uncontrollable according to the center manifold theorem (see for instance, [10]).
- The results in this paper shows the necessity for a truly non-linear controller using both $\{T_g, \beta\}$
- The uncontrollability evidence was shown using real world measurements
- A complete controllability analysis in a generic form using the matrices $\{A, B\}$ is very involved

# 6 Conclusion

In this paper, a complete dynamic model for a wind power turbine has been revised and analyzed. Using Lagrangian mechanics along with aerodynamical modeling a complete non-linear model in state-space was revised.

After a linearization around an equilibrium point with one the control inputs constant $\beta = 3.5$, the complete uncontrollability of the system using only $T_g$ is concluded. Resorting to the center manifold theorem, the local uncontrollability of the non-linear system is shown.

This conclusion encourage a more detailed research using nonlinear controllability and nonlinear controllers like optimal control, piecewise linear controllers and so on. This research, in fact conforms a matter of future work.

*Acknowledgment:*
The authors would like to acknowledge Universidad Tecnológica Nacional, Facultad Regional Bahía Blanca, Departamento de Ingeniería Eléctrica and GESE.

*References:*

[1] Ren, Zhengru and Verma, Amrit Shankar and Li, Ye and Teuwen, Julie JE and Jiang, Zhiyu, Offshore wind turbine operations and maintenance: A state-of-the-art review, *Renewable and Sustainable Energy Reviews*, Vol.144, pp. 110886.

[2] Lubosny, Zbigniew and Lubosny, Z, *Wind turbine operation in electric power systems: advanced modeling*, Springer, 2003.

[3] Van der Hooft, EL and Van Engelen, TG, *Estimated wind speed feed forward control for wind turbine operation optimization*, ECN, 2004.

[4] Simani Silvio, Overview of modeling and advanced control strategies for wind turbine systems, *Energies*, Vol.8, No.12, pp. 13395-13418.

[5] Shwas Abdulhamed and Katebi Reza, Wind turbine control using PI pitch angle controller , *IFAC proceedings volumes*, Vol.45, No.3, pp. 241-246.

[6] Ansoategui, Igor and Zulueta, Ekaitz and Fernandez-Gamiz, Unai and Lopez-Guede, Jose Manuel, Mechatronic modeling and frequency analysis of the drive train of a horizontal wind turbine , *Energies*, Vol.12, No.4, pp. 613.

[7] Meng, Jiayao and Dai, Kaoshan and Zhao, Zhi and Mao, Zhenxi and Camara, Alfredo and Zhang, Songhan and Mei, Zhu, Jose Manuel, Study on the aerodynamic damping for the seismic analysis of wind turbines in operation , *Renewable Energy*, Vol.159, pp. 1224-1242.

[8] Menezes, Eduardo José Novaes and Araújo, Alex Mauricio and Da Silva, Nadege Sophie Bouchonneau, A review on wind turbine control and its associated methods , *Journal of cleaner production*, Vol.174, pp. 945-953.

[9] Gesualdo, Antonio and Iannuzzo, A and Penta, F and Monaco, Michelina, Nonlinear dynamics of a wind turbine tower, *International Journal of Science and Technology*, Vol.14, 2019, pp. 342-350.

[10] Alberto Isidori. Nonlinear Control Systems. Springer. Third Edition. 1997.

## Contribution of Individual Authors to the Creation of a Scientific Article (Ghostwriting Policy)

José Vissio carried out the mathematical model and simulation in Matlab-Simulink.
Andrés García provides advices and support during the mathematical model process and simulation stages.

## Sources of Funding for Research Presented in a Scientific Article or Scientific Article Itself

This work is entirely supported by Universidad Tecnológica Nacional-Facultad Regional Bahía Blanca-Departemento de Ingeniería Eléctrica-GESE. Under the R-D project BBENECI237.

## Conflict of Interest

The authors have no conflicts of interest to declare that are relevant to the content of this article.